World Journal of Engineering and Technology, 2014, 2, 260-268
Published Online November 2014 in SciRes. http://www.scirp.org/journal/wjet
http://dx.doi.org/10.4236/wjet.2014.24027

Scientific Research

Strain Rate Effect on the Response of Blast Loaded Reinforced Concrete Slabs

Kamel S. Kandil[1], Mouhamad T. Nemir[1], Ehab A. Ellobody[2], Ramy I. Shahin[1*]

[1]Department of Civil Engineering, Faculty of Engineering, Menoufiya University, Shibin El Kom, Egypt
[2]Department of Structural Engineering, Faculty of Engineering, Tanta University, Tanta, Egypt
Email: *Ramy.Shahin@Gmail.com

Received 20 July 2014; revised 5 September 2014; accepted 20 September 2014

Academic Editor: Mostafa Morsi Elshami, Structural Engineering, Construction Engineering Department, Faculty of Engineering, University of Dammam, Arabia

Abstract

Dynamic Increase Factor (DIF) due to strain rate effect was examined with documented experimental work done by Razaqpur, *et al.* In the experiment work, two 1000 × 1000 × 70 mm reinforced concrete slabs were constructed. The slabs were subjected to blast loads generated by the detonation of either 22.4 kg or 33.4 kg of ANFO located at a 3.0 m standoff. Blast wave characteristics, including incident and reflected pressures and reflected impulses were measured. The slabs were modeled by explicit analysis with or without strain rate effect to study their behavior under blast load to compare their predicted and observed behavior. The predicted post-blast damage and mode of failure for each model is compared with the observed damage of experimental work. It was concluded that when the dynamic increase factor added to concrete and reinforcement materials due to strain rate effect, the behavior of model under blast load become closer to experimental work.

Keywords

Explicit Analysis, Strain Rate, Blast Load, Ls-Dyna, Scaled Distance

1. Introduction

Since testing of structures under the effect of real explosives requires complex instrumentation and a safe test range, it is not always feasible to carry out a large number of such tests. Therefore, to gain deeper insight into

*Corresponding author.

How to cite this paper: Kandil, K.S., Nemir, M.T., Ellobody, E.A. and Shahin, R.I. (2014) Strain Rate Effect on the Response of Blast Loaded Reinforced Concrete Slabs. *World Journal of Engineering and Technology*, **2**, 260-268.
http://dx.doi.org/10.4236/wjet.2014.24027

the detailed behavior and performance of structures under blast loads, one must resort to analytical and advanced numerical techniques. However, the results of the analysis must be confirmed by some amount of testing to ensure the validity of the assumptions and procedures used in the analysis.

The objective of this paper is to compare the observed behavior of reinforced concrete panels, subjected to nominally similar blast loads, with their predicted behavior using explicit analysis computer program Ls-Dyna for the following material models:

1) Static stress-strain curve for concrete and steel material;

2) Stress-strain curve for concrete and steel material in conjunction with strain rate effect.

Explicit FEM analysis is used to apply incremental procedure for load (or displacement). At the end of each increment, the stiffness matrix based on geometry changes and material changes (if applicable) is updated. Then a new stiffness matrix is constructed, and the next increment of load (or displacement) is applied to the system. This method does not enforce equilibrium of the internal structure forces with the externally applied loads. Therefore, the hope is that if the increments are small enough, the results will be accurate.

When the loading rate is high, the mechanical response of a material is generally different from that at a low loading rate. Such rate dependence is observed for nearly all the brittle materials. Concrete exhibits also an enigmatic phenomenon of increased resistance when it is loaded at a very high rate as explained below.

2. Experimental Work

Seven 1000 × 1000 × 70 mm reinforced concrete slabs (**Figure 1**), were identically doubly reinforced with welded steel mesh of bar cross-sectional area of 25.8 mm^2, and center-to-center spacing of 152 mm in each direction, mass per unit area of 2.91 kg/m^2, yield stress of 480 MPa and ultimate strength of 600 MPa. The concrete had an average 28 day compressive strength of 40 MPa [1].

The slabs designated CS2 to CS4 were as-built while other panels were retrofitted on each face with two sheets of GFRP [1]. This study focused on as-built panels. The free field incident pressure was measured by at least two transducers located, at 3.2 and 5.9 m from the center of each test slab. Reflected pressure was measured 3.1 m from the charge center by four transducers located at the mid-length of the four sides of the slab. An LVDT was used to measure the slab central displacement [1].

To commence the test, the tripod holding the charge was centered above the center of the panel and the charge was hung with a wire. The distance from the center of the charge to the center of the test panel was 3.0 m for all panels. The explosive used was ANFO, comprising 5.7% fuel oil and 94.3% ammonium nitrate, shaped into an approximately spherical form. The explosive energy of ANFO is 3717 kJ/kg, which is 82% of the energy of one kilogram of TNT [1]. **Figure 2** shows a test specimen in place and the tripod holding the charge.

It should be noted that specimen CS4 was subjected to the pressure produced by a 22.4 kg charge while the remaining specimens were exposed to the load caused by the detonation of a 33.4 kg charge. In this study, the results of specimens CS2 and CS3 are considered in the comparison with their counterpart of the predicted explicit analysis, as the post-blast observed damage in the un-retrofitted test panels was available for CS2 and CS3.

In both models, the slab support was assumed to be hinged. Blast loading was calculated using the empirical blast loading functions implemented in the CONWEP code based on TM5-1300 technical manual [2]. Free air detonation of 33.4 kg spherical charge was used. In Ls-Dyna program, this function is available in Blast Load command [3].

3. Model 1

In this model, Kinematic Hardening Cap Model was used for concrete material. The implementation of an extended two invariant cap model, suggested by Stojko is based on the formulations of Simo, *et al*. and Sandler & Rubin [3]. In this model, the two invariant cap theory is extended to include nonlinear kinematic hardening as suggested by Isenberg, Vaughn, and Sandler [3].

One of the major advantages of the cap model over other classical pressure-dependent plasticity models is the ability to control the amount of plastic volumetric strain (dilatency) produced under shear loading. Dilatency is produced under shear loading as a result of the yield surface having a positive slope in $\sqrt{J_{2D}}$-J_1 space, where J_1 and J_{2D} are the first and second invariant of the deviatoric stress respectively, so the assumption of plastic flow in the direction normal to the yield surface produces a plastic strain rate vector that has a component in the volumetric (hydrostatic) direction (see **Figure 3**). In models such as the Drucker-Prager and Mohr-Coulomb, this

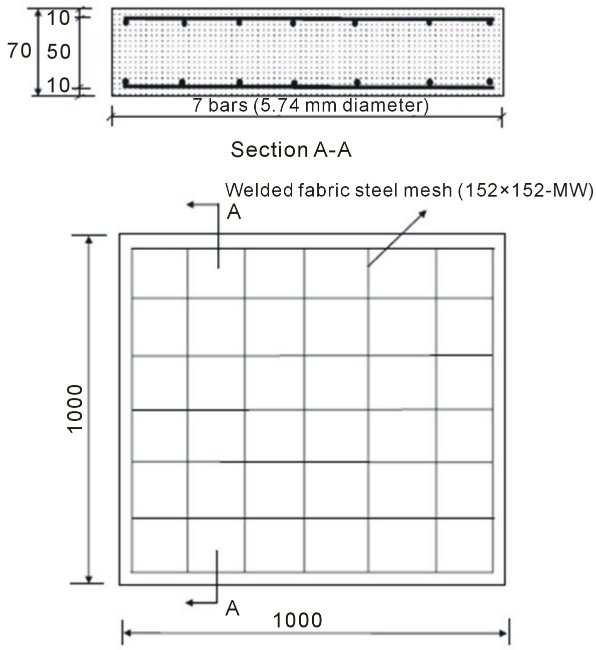

Figure 1. Test specimen geometry and reinforcement details (All dimensions in mm).

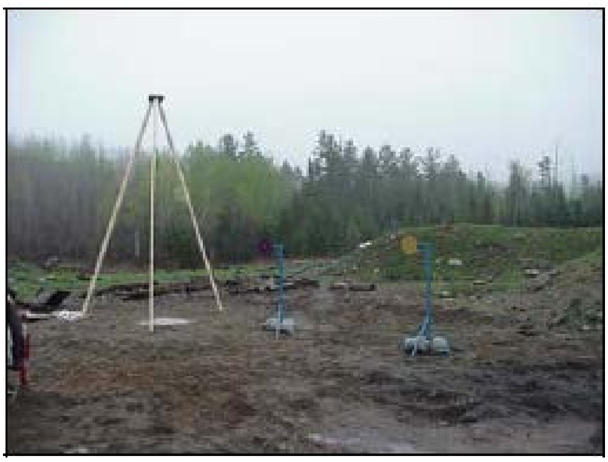

Figure 2. Test specimen with the tripod holding the explosive charge.

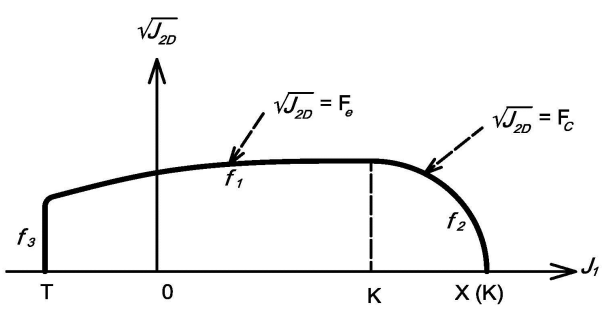

Figure 3. The yield surface of the two-invariant cap model in pressure $\sqrt{J_{2D}}$, J_1 space surface. f_1 is the failure envelope, f_2 is the cap surface, f_3 is the tension cutoff.

dilatency continues as long as shear loads are applied, and in many cases produces far more dilatency than is experimentally observed in material tests. In the cap model, when the failure surface is active, dilatency is produced just as with the Drucker-Prager and Mohr-Columb models.

However, the hardening law permits the cap surface to contract until the cap intersects the failure envelope at the stress point, and the cap remains at that point. The local normal to the yield surface is now vertical, and therefore the normality rule assures that no further plastic volumetric strain (dilatency) is created. In this model, the concrete material fails under principal strain for concrete material. Model 1 is shown in **Figure 4**.

Reinforcement representation in this model was discrete reinforcement in solid elements. Elastic plastic with kinematic hardening material is used for reinforcement bars. The rebar are capable of tension and compression, but not shear (see **Figure 8**).

Experimentally, it was observed on the bottom surface of most panels an array of 500 mm long cracks formed a square shape centered on the panel center and propagated diagonally towards the corners of the panel. Also, cracks inside the square were noted. These cracks are similar to the yield line pattern for a statically applied central patch load. On the bottom surface, additional minor cracks, which typically followed the reinforcement layout, were also observed in experiment work.

Typically, all damaged panels had full depth inverted 45 shear cracks near their supports and on all four sides. These cracks were rather wide and in some cases greater than 4 mm [1].

Analytically, the finite element model fails prematurely. The model show severe damage and most elements failed and deleted. But it is possible to track damage propagation within blast period. On bottom (tension) side, cracks start propagating at support edges (see **Figure 5(a)**). Then, it was also observed an array long cracks formed a square shape centered on the panel center and propagated diagonally towards the corners of the panel (see **Figure 5(b)**). In the next step, adjacent concrete elements crushed within several load steps as well, significantly reducing the local stiffness (see **Figure 5(c)**). In this stage, no need to track cracks in tension face because most elements at tension face were demolished, but it is important to donate that cracks start propagating in the bottom part of compression face as seen in **Figure 5(d)**.

Also, on the bottom surface, cracks followed the reinforcement layout, were also observed, which means that the bond between concrete and steel are demolished.

On the compression face, cracks propagate latterly. Stresses are similar to yield line pattern for a statically applied central patch load (see **Figure 6(a)**). Then, these stresses extended with demolition propagation at the center of panel (see **Figure 6(b)**). Demolition in the center of plate increases as seen in **Figure 6(c)** and cracks start to propagate diagonally from corners (see **Figure 6(d)**). Central cracks array increased in size and diagonal cracks extended to the center of the panel as seen in **Figure 6(e)**.

Finally central cracks were met with diagonal cracks as seen in **Figure 6(f)**. These cracks are extended to the bottom face because the tension side was totally demolished earlier as explained.

Cracks propagation is similar to experimental work as seen in **Figure 13(a)** and **Figure 14(a)**, although cracks in the analytical work are more severe.

Maximum displacement was at the center of plate but it cannot be estimated here because of the total loss for panel stiffness. Complete demolition for concrete plate may refer to the strain rate effect. When the loading rate is high, the mechanical response of a material is generally different from that at a low loading rate.

4. Model 2

In this model, Piecewise Linear Isotropic Plasticity material is used. This material includes strain rate effects [3]. Concrete exhibits an enigmatic phenomenon of increased resistance when it is loaded at a very high rate [4] [5]. To account for strain rate, the stress strain curve for static strain rate "equal to 3.0E−05" is plotted [6]. Then, the Dynamic Increase Factor (DIF), *i.e.* the ratio of the dynamic to static strength, is calculated using CEB formula for compression [7]-[9]. Erosion is added as a way of including failure in these models. In this model, the concrete material fails under principal strain for concrete material (see **Figure 7** for stress strain curve for concrete material under different strain rates).

Elastic plastic with kinematic hardening material is used for reinforcement bars (see **Figure 8**). Strain rate is accounted for using the Cowper and Symonds [3] model which scales the yield stress by a strain rate dependent factor (see **Figure 9** for the meshing of concrete panel).

Experimentally, it was observed on the bottom surface of most panels an array of 500 mm long cracks formed

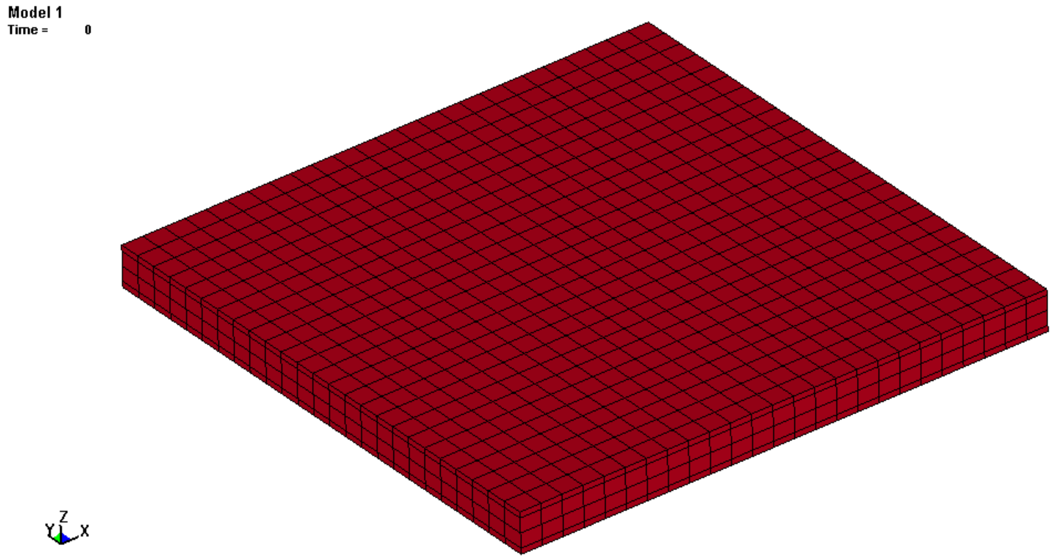

Figure 4. Model 1 using Ls-Dyna program.

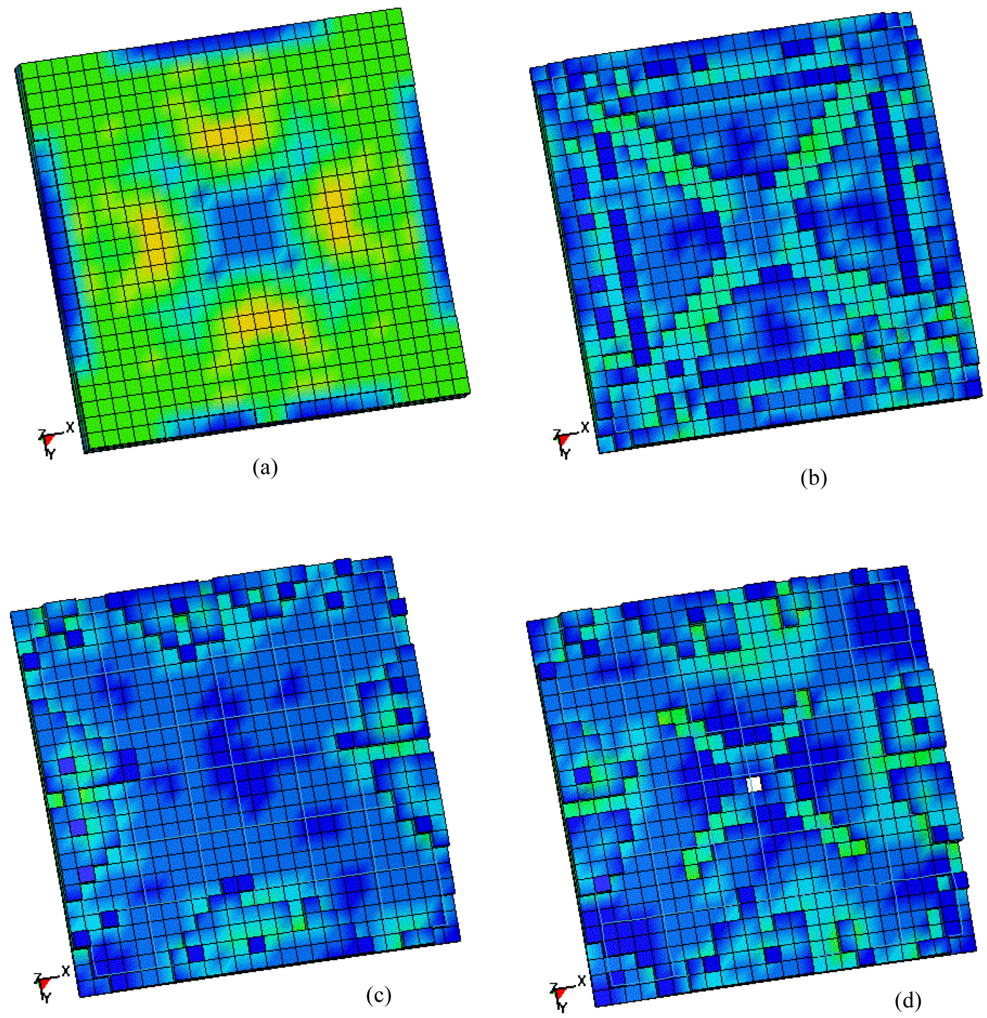

Figure 5. Cracking & crushing propagation at tension face of Model 1.

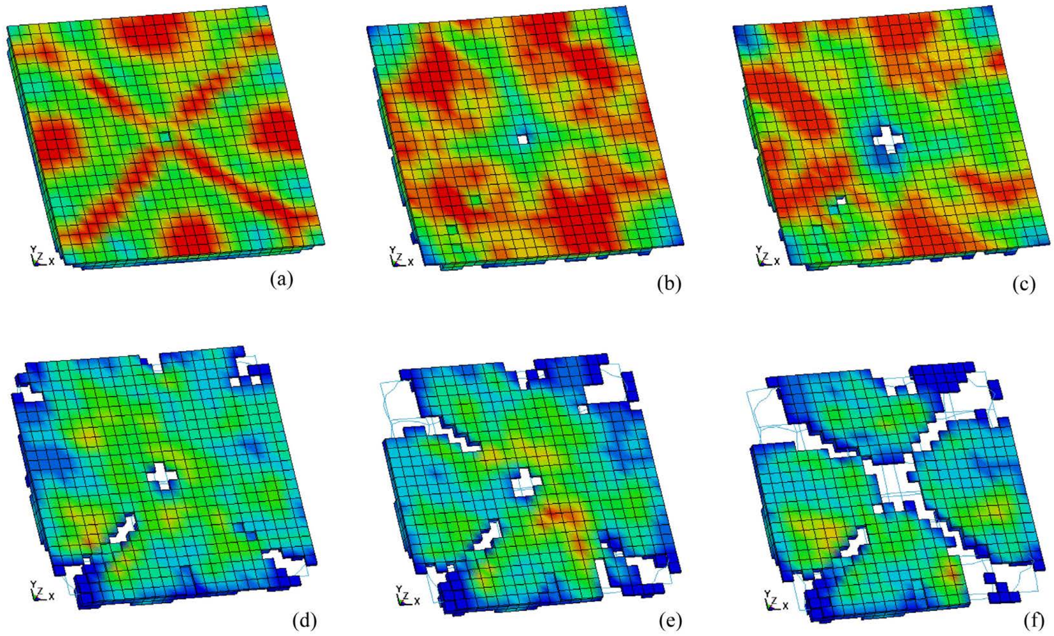

Figure 6. Cracking & crushing propagation at compression face for Model 1.

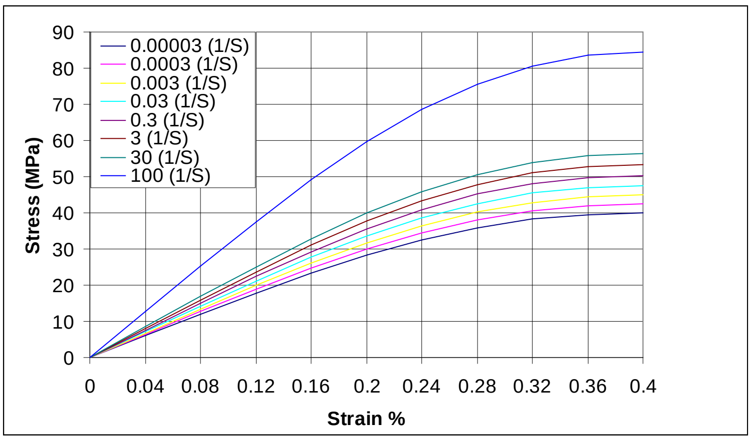

Figure 7. Stress-strain curve for piecewise linear isotropic plasticity concrete material under different strain rates.

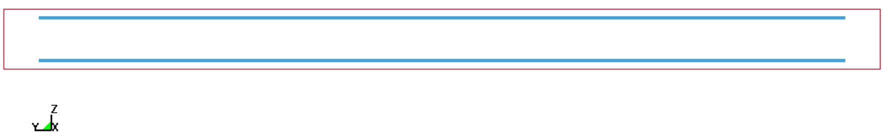

Figure 8. Front view for in the Ls-Dyna Model 1 & Model 2 showing reinforcement bar.

a square shape centered on the panel center and propagated diagonally towards the corners of the panel. Also, cracks inside the square were noted. These cracks are similar to the yield line pattern for a statically applied central patch load.

On the bottom surface, additional minor cracks, which typically followed the reinforcement layout, were also observed in experimental model. Analytically, in the bottom "tension" face, cracks are propagates in center and extend to the edges in the same time (see **Figure 10(b)**). Then, cracks size increased particularly at center and corners of panel (see **Figure 10(c)** and **Figure 11(d)**).

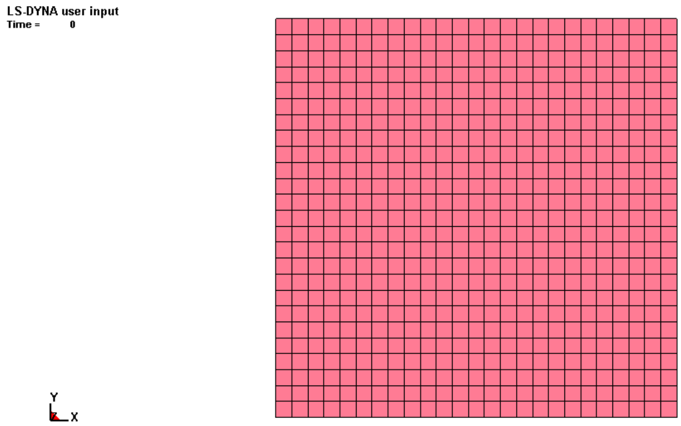

Figure 9. Plan for the Ls-Dyna Model 2 showing meshing for experiment.

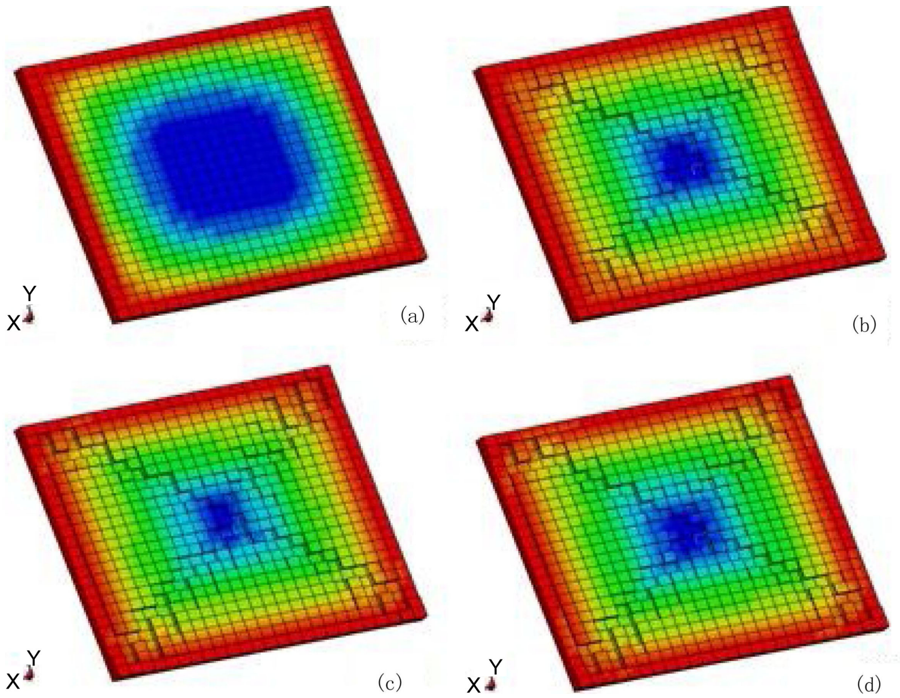

Figure 10. Cracking & crushing propagation at tension face of Model 2.

In the top "compression" face, diagonal cracks are propagated (see **Figure 11(b)**). The size and location of cracks remain unchanged at the end of blast load (see **Figure 11(c)** and **Figure 11(d)**).

In Ls-Dyna model, the size of square shape array is 550 mm long and the damage in yield line region extend to the 50% of the plate thickness. Addition damages are also noted at support boundary (see **Figure 10** and **Figure 11**).

The maximum experimental central deflection for the two identical plates was 13.12 mm for panel CS2 and 9.53 mm for panel CS3, with an average deflection of 11.33 mm. Maximum central deflection in Model 2 was 11.66 mm as seen in **Figure 12** which agree very well with experimental work.

Damage pattern in Ls-Dyna model 2 is more close to experimental work as seen in **Figure 13** and **Figure 14**. This means that the material behavior under high strain rates play an important role in the analytical work.

5. Conclusions

The comparison between the field test results for the slabs subjected to a detonation of 33.4 kg of (ANFO) ma-

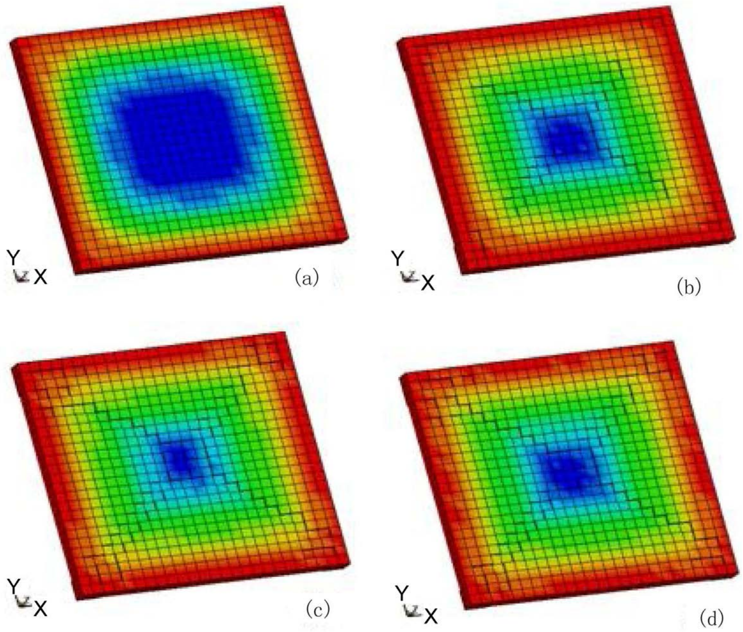

Figure 11. Cracking & crushing propagation at compression face of Model 2.

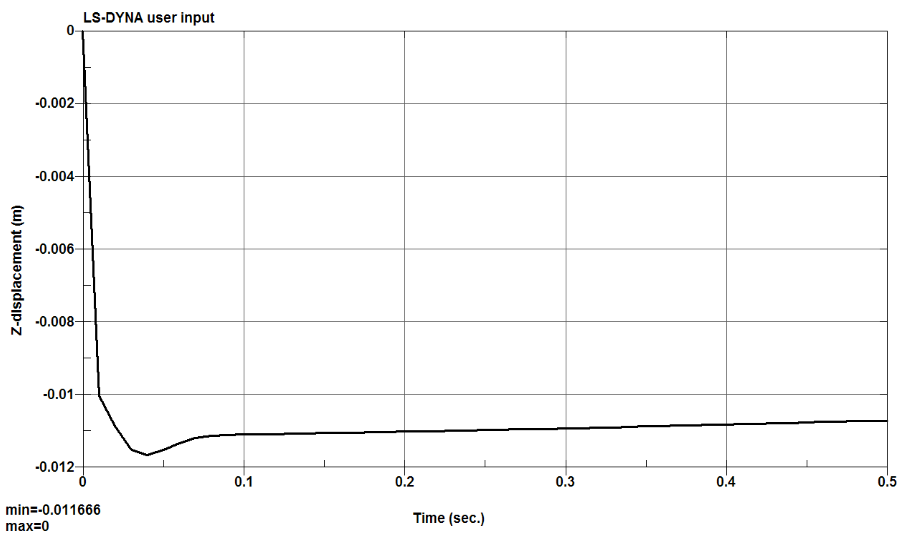

Figure 12. Central time-displacement curve for Ls-Dyna Model 2 in (m).

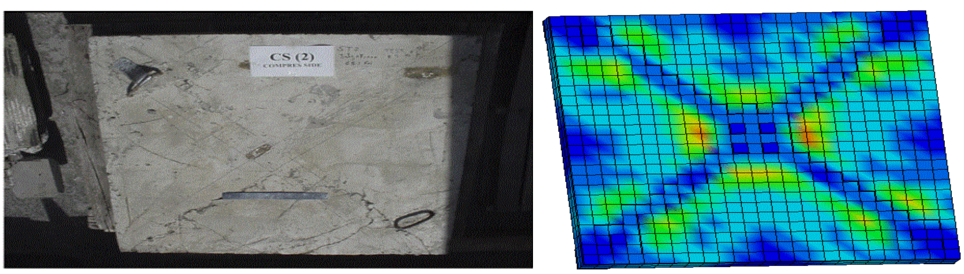

(a) (b)

Figure 13. Model 2 predicted and field observed damage in a typical test slab [top face]. (a) Observed damage; (b) Predicted damage.

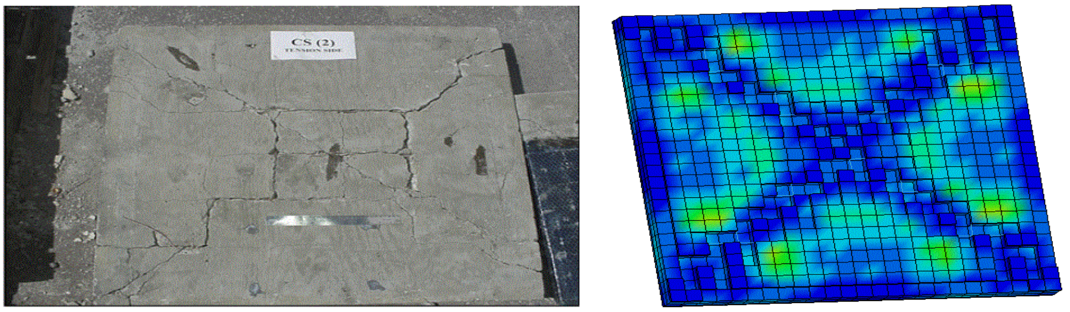

(a) (b)

Figure 14. Model 2 predicted and field observed damage in a typical test slab (bottom face). (a) Observed damage; (b) Predicted damage.

terial generally compared well with the results of the explicit analysis using Ls-Dyna. it is possible to study the model after total failure where the model become unstable, *i.e.* explicit solver provide better presentation for blast load than implicit solver.

It was also concluded that strain rate effect is vital to get good presentation for blast load. Comparison proves that using Dynamic Increase Factor (DIF) for concrete and steel material provides much better presentation. So, it is important to account for dynamic increase factor for concrete and steel material for high strain rate loads such as blast and impact.

References

[1] Razaqpur, A.G., Tolba, A. and Contestabile, E. (2007) Blast Loading Response of Reinforced Concrete Panels Reinforced with Externally Bonded GFRP Laminates. *Elsevier Journal of the Composites*: *Part B*, **38**, 535-546.

[2] TM-5-1300 (1990) Design of Structures to Resist the Effects of Accidental Explosions. US Department of the Army Technical Manual, Washington DC.

[3] Hallquist, J.O. (2003) Ls-Dyna Theoretical Manual. Livermore Software Technology Corporation, California.

[4] Faust, B. (2000) Evaluation of the Residual Load-Bearing Capacity of Civil Structures Using Fuzzy-Logic & Decision Analysis. University of the Federal Army, Neubiberg.

[5] Lu, Y. and Xu, K. (2004) Modeling of Dynamic Behaviour of Concrete Materials under Blast Loading. *International Journal of Solids and Structures*, **41**, 131-143.

[6] Ellobody, E. and Bailey, C.G. (2008) Behaviour of Unbonded Post-Tensioned One-Way Concrete Slabs. *Reprinted from Advances in Structural Engineering*, **11**. (Multi-Science Publishing CO. LTD, UK)

[7] Malvar, L.J. and Crawford, J.E. (1998) Dynamic Increase Factors for Concrete. 28*th DDESB Seminar*, Orlando, September 1998.

[8] Moon, N.N. (2009) Prediction of Blast Loading and Its Impact on Buildings. Master of Technology in Civil Engineering Thesis, National Institute of Technology, Rourkela.

[9] Ngo, T., Mendis, P., Gupta, A. and Ramsay, J. (2007) Blast Loading and Blast Effects on Structures—An Overview. *EJSE Special Issue*: *Loading on Structures*, 76-91.